A Max 349 GHz 18.2mW/Pixel CMOS Inter-modulated Regenerative Receiver for Tri-Color mm-Wave Imaging

Adrian Tang[1], Qun Gu[2], Zhiwei Xu[3], Gabriel Virbila[1] and Mau-Chung Frank Chang[1]

[1] Univ of California, Los Angeles, Los Angeles, CA, [2] Univ. of Florida, Gainsville, [3] HRL Labortories, Malibu, CA

***Abstract* — This paper presents a mm-wave imaging CMOS regenerative receiver which is intermodulated by a second oscillator to provide multiple receive bands at 349, 201 and 53 GHz for false color imaging. The proposed receiver consumes 18.2mW per pixel and occupies 0.021mm^2 of silicon area.**

I. INTRODUTION

Sub-mm-wave and mm-wave based imaging has recently gained interest for security screening and bio-imaging applications. As a response to this interest, the circuit community has proposed several approaches to implement mm-wave imaging systems in CMOS technology [1,2,3]. While these approaches meet the major challenges of noise, sensitivity and dynamic range, they are all narrowband approaches (single frequency) and suffer from narrowband imaging effects including edge ghosting, speckle, and a limited ability to discriminate between different materials in the scene [4]. For mm-wave imaging to become practical, high operating frequencies are also necessary as the operating frequency limits the attainable spatial or "cross" resolution (wavelength dependent).

The major advantage offered by CMOS imaging over III-V approaches is the possibility of constructing full 2D imaging arrays. Currently, III-V's pixel performance remains dominant over reported CMOS imaging pixels at the cost of higher power and more area. To take full advantage of the opportunities CMOS technology presents, the pixel circuits employed must offer low pixel area and low power in order to make array integration possible. CMOS imaging receivers based on the principle of super-regeneration have appeared in which an oscillator's start up time is perturbed by an active imaging signal, and a resulting time difference is detected [5]. While this technique provides low area overhead and power performance compared with other techniques, it is still narrowband with an upper frequency limited by Fmax, (highest frequency with device gain available).

II. INTERMOD. REGENERATIVE RECEIVER

In order to directly address these two limitations, we propose the inter-modulated regenerative receiver (IRR) architecture, with block diagram shown in Fig. 1. The proposed IRR can concurrently receive in multiple-bands to approximate a broadband image. In this architecture a regenerative receiver at 201 GHz is first constructed with a conventional quench signal. A lower frequency tone is then directly injected from an auxiliary oscillator (aux-osc) at 148 GHz. Unlike the regenerative oscillator (reg-osc), which is periodically quenched at 1 GHz, the aux-osc runs continuously. As the reg-osc is highly non-linear, the injection of the aux-tone creates inter-modulation between both frequencies within the regenerator and gives rise to additional receive bands.

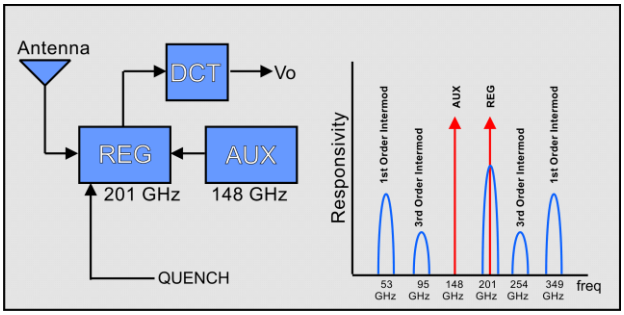

Fig. 1. Inter-modulated regenerative receiver (IRR) architecture showing aux-osc, reg-osc, envelope detector, and key frequencies.

The first order inter-modulation components (53 and 349 GHz) are particularly interesting for imaging as they offer responsivities and noise equivalent powers (NEP) within an order of the fundamental. Also of interest is that the upper inter-modulation component (349 GHz) can be designed to lie well above Fmax (250 GHz for 65nm), which allows the receiver to operate beyond frequencies where device gain is available, a phenomenon not possible with any other conventional receiver topology.

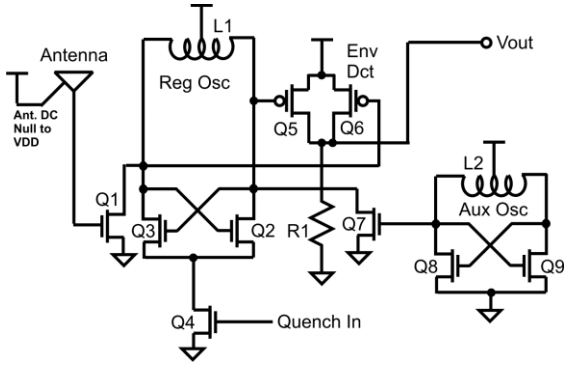

Fig. 2. Inter-modulated regenerative receiver (IRR) CMOS circuit implementation.

The upper limit on the oscillation frequency of the reg-osc remains Fmax to sustain oscillation, while the limit on the aux-osc is more complicated. If the aux frequency is placed too close to the regenerative frequency, the two oscillators may become injection locked, and the mechanism for generating

978-1-4673-1088-8/12/$31.00 ©2012 IEEE

multiple bands will be defeated. Also note that it is possible to receive on higher order inter-modulated frequencies, nevertheless responsivity and NEP would be limited.

Fig. 2 details the circuit implementation of the IRR in a 65nm CMOS technology. Q1 has no gain but prevents the low impedance antenna from loading the reg-osc. Q2, Q3, and L1 form the reg-osc which is periodically quenched by the current source Q4. Q8, Q9, and L2 form the aux-osc that provides the injected tone through current injection device Q7. Q5, Q6, and R7 form an envelope detector that converts the reg-osc envelope into a base-band output signal. Note that there is no matching structure between the antenna and Q1. For such broadband application (50 to 350 GHz) any matching structure inserted would make little sense. Instead we rely on the high gain of the regenerative stage to overcome the loss and still provide the needed performance.

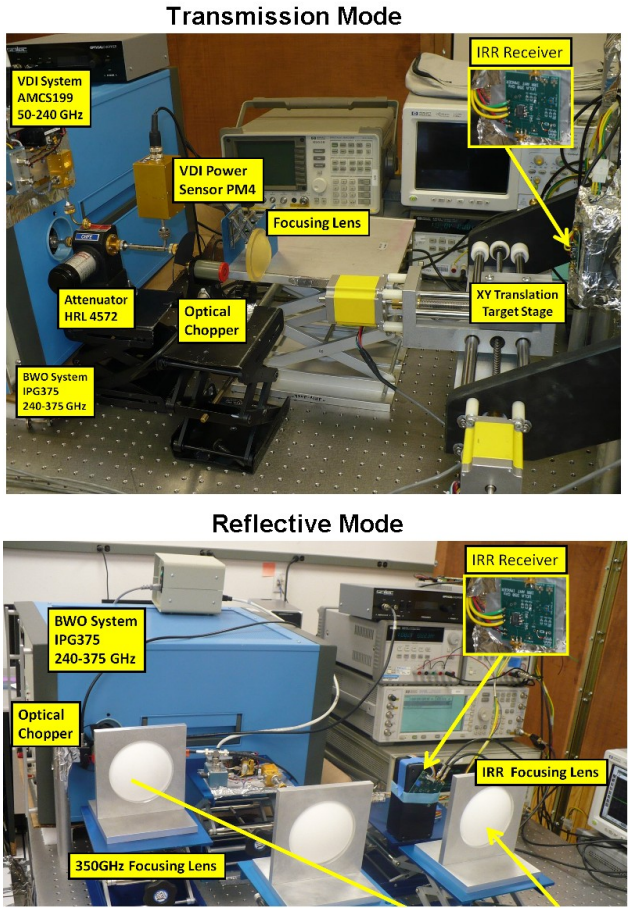

Fig. 3. Test setup showing BWO source (349 GHz), VDI source (53 & 201 GHz) and XY stage used for both transmission mode imaging and reflective mode imaging.

III. MEASUREMENTS

By using the setup shown in Fig. 3, the responsivity and NEP of the proposed IRR architecture are quantified. In the test setup a BWO (backwards-wave oscillator) is employed to test the 349 GHz band while an AMC (active multiplier chain) from VDI Inc. is used to characterize the 53 and 201 GHz bands. An attenuator and power meter are placed at each source output while the receiver is placed at a distance and focused on with a lens. The output voltage of the IRR is recorded as power is swept while voltage noise floor is measured with a spectrum analyzer. Finally the IRR and power meter position are exchanged so the path loss can be measured to obtain the true power incident on the IRR. The responsivity and NEP of each band at each power level is plotted in Fig 4. Note that although the inter-modulated bands exhibit lower performance than the fundamental, they are still quite competitive with other detector and receiver approaches. Interesting to note is that the IRR provides a lograthmic response which is the opposite of the exponential response of most detectors. This is actually desirable for imaging as the gain and noise performance are orders of magnitude better at lower power levels where reflective imaging systems operate.

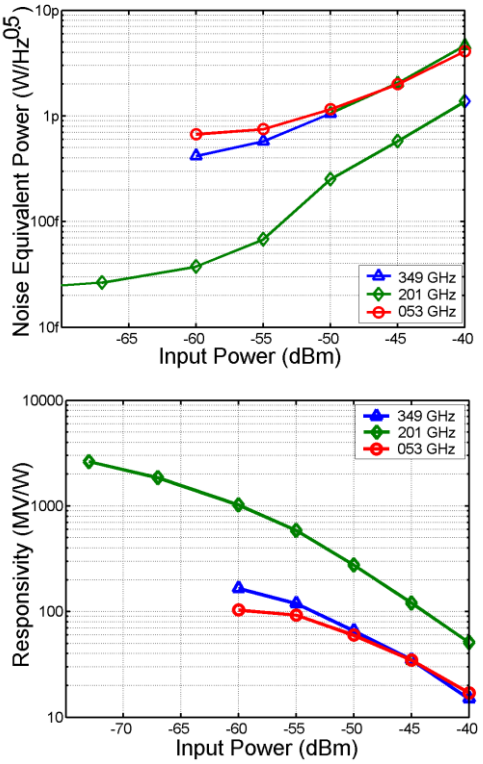

Fig. 4. Measured NEP and responsivity vs. power level for 53, 201, and 349 GHz bands of the inter-modulated regenerative receiver (IRR).

To demonstrate transmission-mode imaging operation an XY translation stage is placed between the IRR and each source as shown in Fig. 3. A target (stuffed bear and bottle) is placed on the stage and scanned. The scan is performed at 3 different frequencies (53,201, and 349 GHz), and the results are assigned 3 false colors based on the wavelengths as shown in Fig. 5. While each narrowband scan only provides limited scene information the composite image provides much better discrimination between materials. For example the bear is sitting on a styrofoam block, which offers the dominant transmission coefficient at low frequencies, and so the red 53 GHz is the dominant color over the other channels. The bear's nose is mostly yellow and lacks blue meaning the 349 GHz band is heavily attenuated. The body region seems to transmit

978-1-4673-1088-8/12/$31.00 ©2012 IEEE

best at the green 200 GHz band. Note all 3 source powers and responsivity are equalized to the same value by using external DSP to provide fair relative contrasts in the final image. The reflective setup shown in Fig. 3 was used to capture the reflective images in shown Fig. 6. For reflective mode imaging, only the 349 GHz band is used as the smaller 53/201GHz AMC does not provide enough power to overcome the high reflective path loss of the 1.2 m target distance and the optical losses of the lenses.

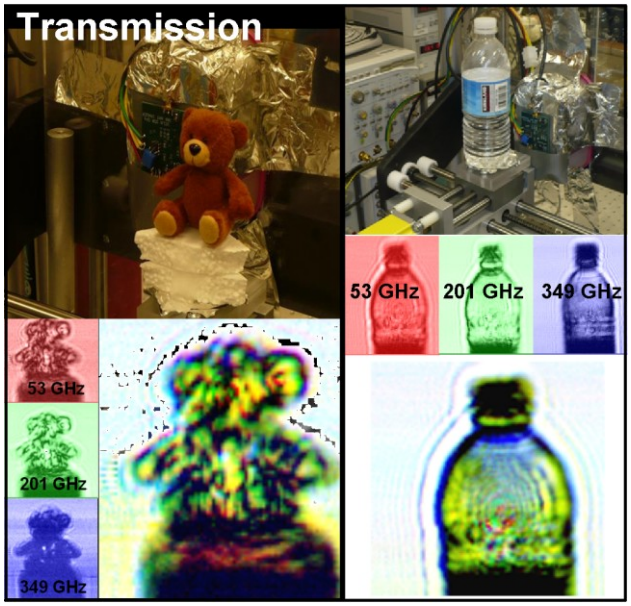

Fig. 5. Color transmission mode imaging (captured through three receiving bands at 53, 201, 349 GHz) of a stuffed bear and water bottle.

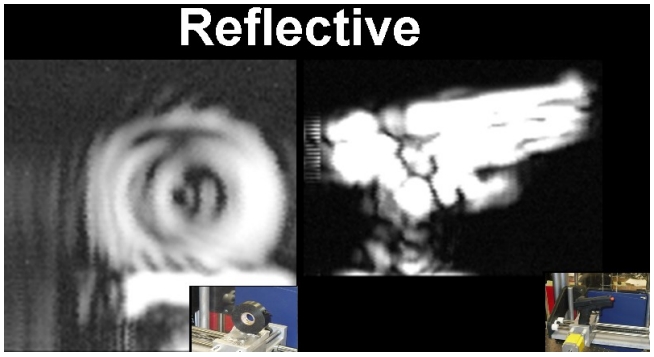

Fig. 6. Reflective image captures of a roll of tape and replica handgun at 349 GHz.

The IRR receiver performance is summarized in Tab. 1 along with a comparison to other state-of-art mm-wave imaging receivers. The IRR is unique in offering 3-color images in transmission mode and is the first CMOS system with enough sensitivity for reflective mode with reasonable integration times. Compared with other super-regenerative approaches [5] the frequency, power and area are competitive, but with the addition of multiple bands. The total IRR power dissipation was measured at 18.2mW/pixel. The IRR occupies 0.45 mm2/pixel of area including antenna. Fig. 7 shows the IRR die photo implemented in 65nm CMOS with an on-chip antenna.

Receiver Characteristics	Value
Simultaneous Receiving Frequency Bands	53, 201, and 349 GHz
Power Dissipation	18.2mW / pixel
Pixel Die Area	0.45 mm^2 (0.021 without antenna)
349 GHz Band Peak Responsivity	187 MV/W
201 GHz Band Peak Responsivity	2650 MV/W
53 GHz Band Peak Responsivity	103 MV/W
349 GHz Noise Equivalent Power	405 fW / $Hz^{0.5}$
201 GHz Noise Equivalent Power	28 fW / $Hz^{0.5}$
53 GHz Noise Equivalent Power	665 fW / $Hz^{0.5}$

RX Characteristic	[1] JSSC 2009	[2] RFIC 2010	[3] CICC 2007	[5] ISSCC 2011	This Work
Image Color(s)	Black/White	Black/White	Black/White	Black/white	3 False Colors
Receiving mode(s)	Transmission	Passive	Transmission	Transmission	Transmission & Reflective
Power Dissipation (mW/pixel)	5.5	200	93	13.5	18.2
Area (mm^2)	0.03	1.25	0.31	0.013	0.021
NEP (fW /	300000	10.3	200	1.51	405 / 28 / 665
Frequency	600	94	94	183	349 / 201 / 53
Technology	0.25 CMOS	180nm SiGe	65nm CMOS	65nm CMOS	65nm CMOS

Table 1. Performance summary and comparison with other silicon mm-wave imaging receivers.

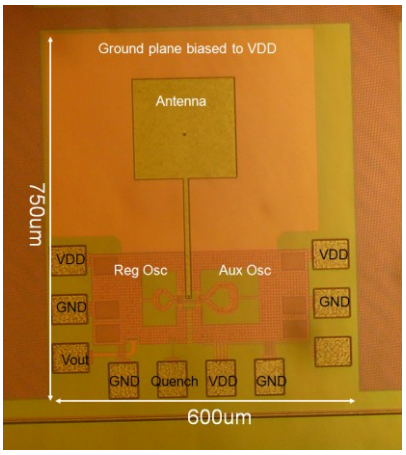

Fig. 7. Die-photo of IRR receiver with on-chip patch antenna. Internal circuits and pads are identified..

REFERENCES

[1] Erik Ojefors, Ullrich R.Pfeiffer, Alvydas Lisauskas, Hartmut G. Roskos, "A 0.65 THz Flocal-Plane Array in a Quarter-Micron CMOS Process Technology", IEEE JSSC, Vol. 44, No. 7, July 2009, pp 1968-1976

[2] Gilreath L, Jain V, Hsin-Cheng Yao, Le Zheng, Heydari, P, "A 94-GHz passive imaging receiver using a balanced LNA with embedded Dicke switch", IEEE RFIC, May2010, pp 79-82

[3] Tang, K.W, Khanpour M, Garcia P, Gamier, C, Voinigescu, S.P, "65-nm CMOS, W-Band Receivers for Imaging Applications", IEEE CICC, Sept. 2007, pp 749-752

[4] Ken B. Cooper, Robert J. Dengler, Nuria Llombart, Tomas Bryllert,Goutam Chattopadhyay, Erich Schlecht, John Gill, Choonsup Lee, Anders Skalare, Imran Mehdi, and Peter H. Siegel "Penetrating 3-D Imaging at 4 and 25m Range Using a Submillimeter-Wave Radar" IEEE MTT, Vol 56, No. 12, Dec 2008, pp 2771-2778

[5] Adrian Tang and Mau-Chung Frank Chang, "183GHz 13.5mw/pixel CMOS Regenerative Receiver for mm-wave imaging applications", IEEE ISSCC, Vol 54, Feb. 2011, pp 296-297

978-1-4673-1088-8/12/$31.00 ©2012 IEEE